THERMAL WAVES OR BEAM HEATING IN THE 1980, NOVEMBER 5 FLARE

Dean F. Smith

Berkeley Research Associates
Berkeley, California
and
Department of Astrophysical, Planetary and Atmospheric Sciences
University of Colorado
Boulder, Colorado

ABSTRACT

Observations of the temporal evolution of loop BC in soft X rays in the November 5, 1980 flare are reviewed. Calculations are performed to model this evolution. The most consistent interpretation involving a minimum account of energy is the following. Thermal heating near B gives rise to a conduction front which moves out along the loop uninhibited for about 27 s. Beam heating near C gives rise to a second conduction front which moves in the opposite direction and prevents any energy reaching C by thermal conduction from B. Thus both thermal waves and beam heating are required to explain the observed evolution.

1. INTRODUCTION

Two analyses have been performed for the heating and subsequent evolution of loop BC in the 1980, November 5 flare. The first was a beam heating calculation by Duijveman, Somov and Spektor (1983; hereafter DSS). They showed that beam heating could not explain the observed large increase in density of the loop during the flare which requires continuous energy and/or mass input after the impulsive phase. The second was an investigation of observations supporting a thermal wave interpretation by Rust, Simnett and Smith (1985; hereafter RSS). They used observations of a weak contour from bands 1-3 (3.5-11.5 keV) of the Hard X-ray Imaging Spectrometer (HXIS) to infer the presence of a conduction front moving out from B along loop BC. It was noted in RSS that the electron beam of DSS arrived at point C at about 22:33 UT and thus the contours immediately after this time could be influenced by a beam component.

Our approach is to examine the observations to determine what constraints they place on a model. We employ our flux-corrected transport (FCT) code (Smith and Harmony 1982) to model cases of normal heating and beam heating using the model loop of DSS as described in Section 3. The latest results of the laser-fusion community on heat transport in steep temperature gradients (Smith 1986) are employed in our code. The results presented in Section 4 show that thermal conduction and thermal waves play an important role in all cases, but not as dominant a role as could be inferred from RSS. A discussion of these results and their implications is given in Section 5.

2. OBSERVATIONS

We divide the observations into three phases. The first phase is the preflare phase up to HXIS image 152 or 22:32:29 UT. The second phase is an expansion phase from 22:32:29 to 22:33:16 which coincides with the images used by RSS to infer thermal waves (Figure 1b). The third phase is a slow continuation of this expansion contemporaneous with another expansion from footpoint C which eventually results in their merging from 22:33:16 to 22:34:31. We consider these phases in turn.

The first phase is of interest mainly for determining appropriate initial temperatures and densities in loop BC. The end time of the 4.5 s accumulation interval corresponding to frame 152 is 22:32:29. DSS present in their Table II values for the density and temperature at an earliest time of 22:32:50 averaged over ±1 min at the top of the loop and footpoint C. The problem with this procedure is that the flare had already started for a significant fraction of this interval as is clear from Figure 2 of DSS so that the temperatures are not indicative of the preflare state. Machado (private communication) obtained temperatures over the interval 22:30 to 22:31 and found 12×10^6 K for footpoint C and 13×10^6 K for the top of the loop, but with a lower counting rate. Thus, assuming an isothermal loop at 12×10^6 K is a good approximation. The density of 5×10^9 cm^{-3} for both footpoint C and the top of the loop is almost the same as in DSS as would be expected since the amount of heating included in DSS only leads to a substantial density increase sometime beyond 22:32:50.

The observations of the initial expansion phase are shown in Figure 1. Figure 1a includes bands 1 and 2 (3.5-8 keV) with a single 6.7 counts s^{-1} contour whereas Figure 1b includes bands 1-3 (3.5-11.5 keV) and has 2.2, 4.4, 9, and 18 counts s^{-1} contours. The 4.4 counts s^{-1} contour of Figure 1b should correspond closely with the single 6.7 counts s^{-1} contour of Figure 1a. While there is a rough correspondence, it is clear that the addition of band 3 in Figure 1b results in additional smoothing not present in Figure 1a. This throws doubt on the procedure of including band 3 because the number of counts in band 3 should be small compared to the number in bands 1-2 in a purely thermal model for the $10\text{-}30\times10^6$ K temperature range of interest.

A larger problem with a simple thermal wave interpretation of Figure 1b is found by comparing it with Figure 1a. If the weak 2.2 counts s^{-1} contour of Figure 1b was really the result of a thermal wave, then we would expect (Brown et al., 1979; Smith and Harmony, 1982; hereafter SH) that the more intense 6.7 counts s^{-1} contour of Figure 1a should tend to follow the weak contour of Figure 1b. The reason is that a thermal wave is driven by the hot plasma behind it which continues to expand unless there is some very dense cool material like the chromosphere to stop it. There is a complication because the optical depth through the loop varies along the loop, but on purely geometrical grounds, one would expect about 47% as much emission from a pixel at the top of the loop as from one at a footpoint for an isothermal constant density loop near the center of the disk as for the November 5 flare (MacKinnon, Brown and Hayward 1985). Thus at least the 4.4 counts s^{-1} contour of Figure 1b should follow the 2.2 counts s^{-1} contour because the wave only becomes visible some distance along the loop and the expected optical depth variation would be much less than a factor of 2 over significant sections of the tongue of the 2.2 counts s^{-1} contour in the 22:33:16 image.

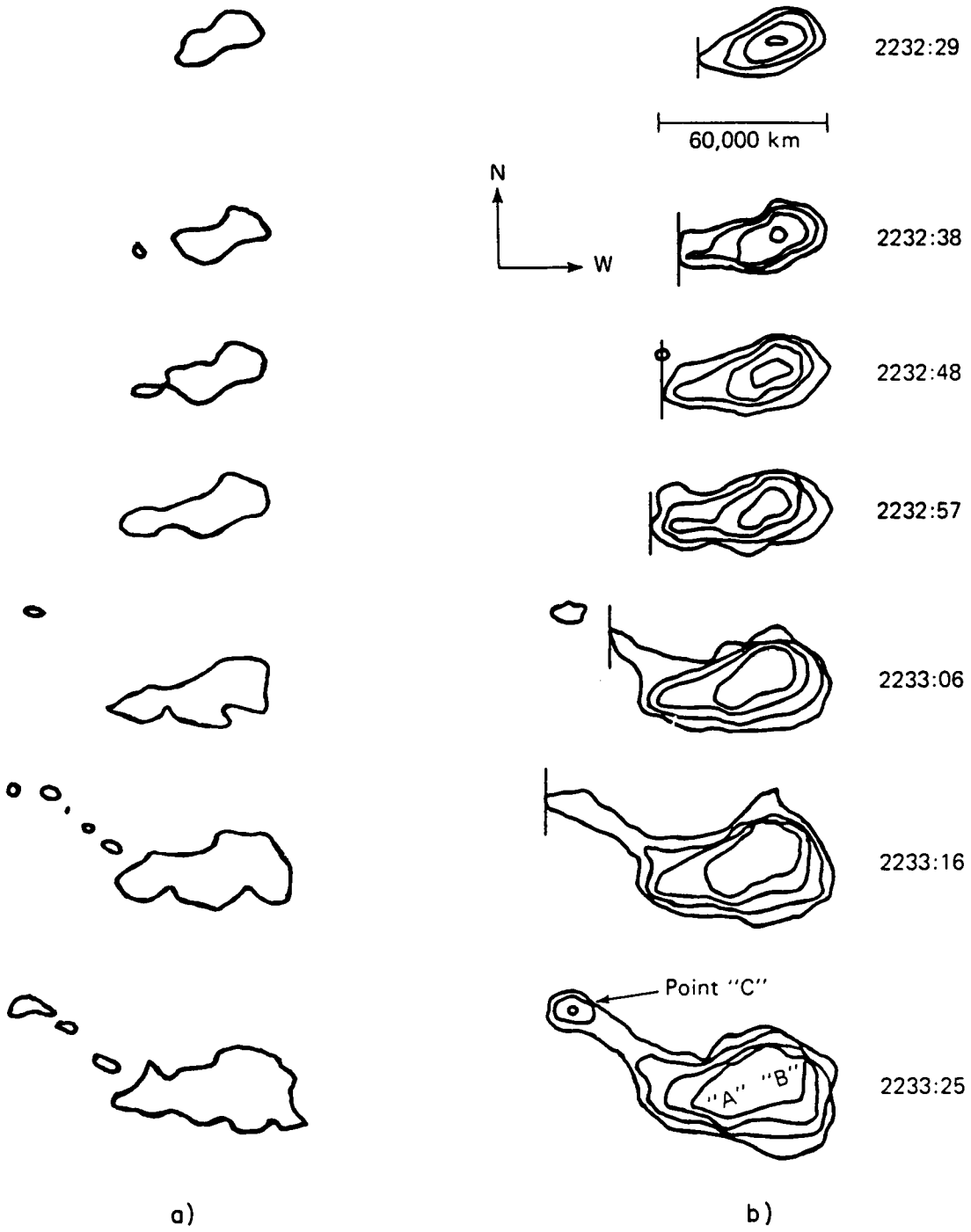

Figure 1. (a) HXIS bands 1 and 2 (3.5-8 keV) at the 6.7 counts $pixel^{-1}$ s^{-1} contour for the times shown at the far right on November 5, 1980. (b) HXIS bands 1-3 (3.5-11.5 keV) at the 2.2, 4.4, 9 and 18 counts $pixel^{-1}$ s^{-1} contours for the same times as (a).

Although there is some indication of the extension of the 4.4 counts s^{-1} contour in this image, it is much less pronounced than would be expected for a pure thermal wave.

Loop BC was there several hours before the flare and continued to exist for several hours after the flare. This implies that whatever caused the X-ray brightening of the loop did not significantly change the gross configuration of the loop and thus it should be sufficient to consider energy transport processes to explain the brightening.

3. MODEL AND METHOD

The model loop used is the same as in Figure 3 of DSS, i.e. a semicircular loop of radius 35,000 km. The total length of the loop is 10^5 km including an extension into the chromosphere as in SH with an initial coronal density of 5×10^9 cm^{-3} and an initial coronal temperature of 5.1×10^6 K. The loop is divided into 900 cells of length 111.1 km. The equations solved are the same as in SH, and the boundary conditions at the coronal end $x = 0$ were

$$v = 0; \quad \frac{\partial T_e}{\partial x} = \frac{\partial T_i}{\partial x} = \frac{\partial \rho}{\partial x} = 0,$$

where v is the velocity, T_e and T_i are the electron and ion temperatures, respectively, and ρ is the total mass density.

The boundary conditions at $x = 10^5$ km were

$$\frac{\partial \rho}{\partial x} = \frac{\partial v}{\partial x} = \frac{\partial T_e}{\partial x} = \frac{\partial T_i}{\partial x} = 0.$$

Ionization equilibrium is assumed to calculate the radiative losses as discussed in SH.

The heat flux Q was calculated in the manner appropriate for steep gradients in which the fast electrons have mean free paths much larger than the temperature scale height (Smith 1986). This has the effect of reducing the heat flux relative to the classical Spitzer-Harm value without anomalous effects such as ion-acoustic waves. Treating the physics adequately leads to the reduction automatically and there is no enhanced electron-ion coupling ($C_{te} = C_{ti} = 0$ in the terminology of SH).

The source term S is taken in one of the two following forms. For thermal heating

$$S = \frac{F(t)}{(2\pi)^{\frac{1}{2}}\sigma(t)} \exp\left[-x^2/2\sigma^2(t)\right], \tag{1}$$

where

$$F(t) = \frac{t}{t_o} J \quad (t < 0.1 \text{ s}),$$

$$F(t) = J \quad (t \geqslant 0.1 \text{ s}),$$

where t_o = 0.1 s, and J is the energy input. For beam heating S is of the form (Emslie 1978)

$$S = K\Lambda n(\delta-2)G(t)E_c^{\delta-2}\int_{E^*}^{\infty}(E_o^{-(\delta+1)}dE_o)/[1-\frac{3K\Lambda N(x,t)}{E_o^2}]^{2/3}, \quad (2)$$

where the beam flux distribution (electrons cm^{-2} s^{-1} per unit E_o) is of the form

$$F(E_o,t) = (\delta-2)\frac{G(t)}{E_c^2}\left(\frac{E_o}{E_c}\right)^{-\delta}, \quad E_o \geq E_c; \quad (3)$$

$K = 2\pi e^4$, Λ is the Coulomb logarithm, n is the density, N(x,t) is the transversed particle column depth, E_c is the cutoff energy, δ is the spectral index and $E^* = \max(E_c,(3K\Lambda N)^{1/2})$. Here G(t) is given by

$$G(t) = \frac{t}{t_o}F \quad (t < 0.1 \text{ s}),$$

$$G(t) = F \quad (t > 0.1 \text{ s}),$$

where F is the energy flux of the beam in ergs cm^{-2} s^{-1}.

For even integer values of δ, the integral in equation (2) is analytic and the results for $\delta = 4$, which is the only value that will be used here, are given in Nagai and Emslie (1984). Equation (2) gives the result for a directed beam. It is a straightforward matter to derive the result for an isotropic beam, but we do not present it because the minimum E_c to propagate a significant amount of energy to footpoint C with a directed beam over the 10^5 km loop with $n = 5\times10^9$ cm^{-3} is 20 keV. It would be significantly higher in the case of an isotropic beam.

The X-ray emission due to both the beam and the heated plasma were calculated at 4 and 8 keV corresponding to energies in bands 1 and 2 of HXIS using standard equations (see, e.g., Emslie 1980; Emslie and Vlahos 1980). For the emission from the beam the results for photon energies $\epsilon < E_c$ must be used. The results in photons cm^{-2} s^{-1} erg^{-1} cm^{-1} refer to a 1 cm thick slab of source. To obtain the total emission we would have to integrate over the line of sight through the loop. This step is beyond the scope of this paper, but it needs to be kept in mind in interpreting the results.

4. RESULTS

The results shown in Figures 2-5 can be divided into the results for thermal heating and emission and the results for beam heating and emission. We consider these in turn. The initial σ used for thermal heating was 3500 km. In Figure 2 the solid lines show a typical conduction front moving out along the loop with a speed ~5 c_s, where c_s is the ion-sound speed. The highest temperature of $\sim30\times10^6$ K is about the temperature DSS deduced for the top of the loop averaging over ±1 min around 22:32:50. The speed of the

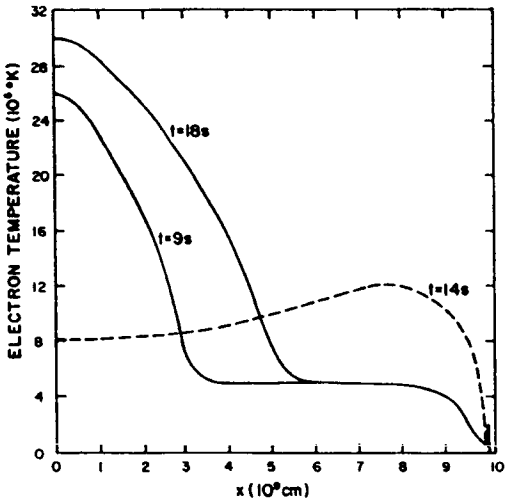

Figure 2. The electron temperature versus distance along the loop for thermal heating with an input of 11.4 erg cm^{-3} s^{-1} for two times (solid lines) and beam heating with an energy flux of 10^{10} erg cm^{-2} s^{-1} (dashed line) which corresponds exactly to the level of thermal heating.

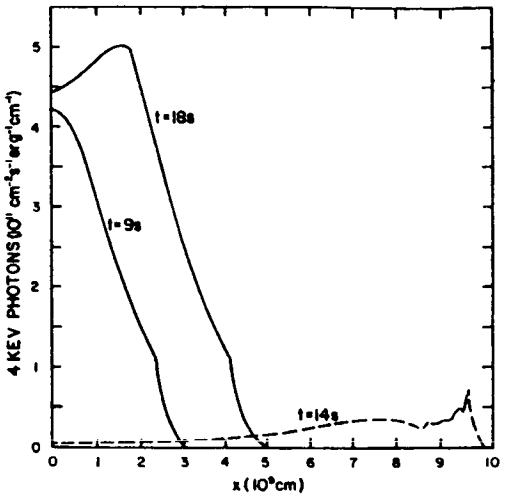

Figure 3. The X-ray emission per unit length (dI/dx) at 4 keV at the source versus distance for thermal heating (solid lines) and beam heating (dashed lines). Only the X-ray emission due to heating is shown for the beam.

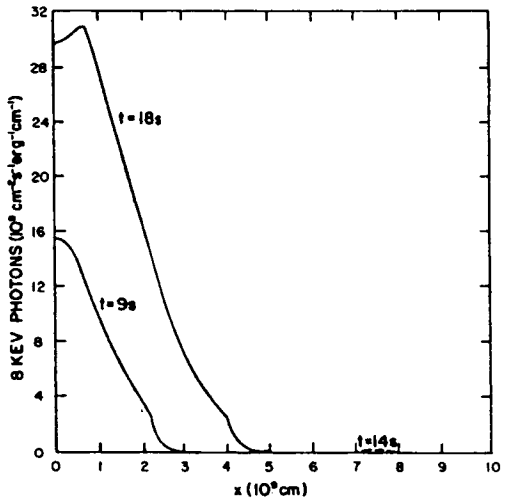

Figure 4. The X-ray emission per unit length (dI/dx) at 8 keV at the source versus distance for thermal heating (solid lines) and beam heating (dashed lines). Only the X-ray emission due to heating is shown for the beam.

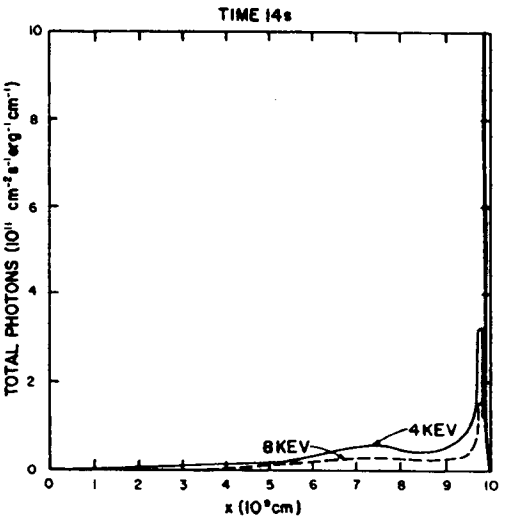

Figure 5. The total X-ray emission per unit length at the source versus distance for a beam. The 4 keV emission (solid line) has a peak off the scale at 24.8×10^{11} photons cm^{-2} s^{-1} erg^{-1} cm^{-1} and the 8 keV emission (dashed line) has a peak off the scale at 12.4×10^{11} photons cm^{-2} s^{-1} erg^{-1} cm^{-1}.

front is ~2.2×10^8 cm s^{-1} which means that, without anything to stop it, the front would run into footpoint C in about 45 s.

However, a conduction front will only continue to move forward if the temperature of the plasma ahead of the front is lower than the temperature of the plasma behind the front. We know that a beam was impacting footpoint C from 22:32:50-22:33:20 because of the impulsive 16-30 keV signature (DSS) which leads to the brightenings in Figure 1a,b at 22:33:06 and some time beyond. This leads to heating as shown by the dashed line in Figure 2 which at t = 14 s would correspond approximately to the 22:33:06 image in Figure 1. This heating would prevent any energy from conduction reaching footpoint C until long after (> 1 minute) beam heating had stopped since it is very unlikely that temperatures higher than those due to beam heating would be produced by a conduction front so far from the region of energy input without producing temperatures near x = 0 much higher than those observed. Because of computer time limitations, we were not able to show this explicitly. It should also be noted that the times in Figures 2-4 are referenced to the start times of two independent calculations, one for thermal heating (solid lines) and one for beam heating (dashed line). Again, because of computer time limitations we made no attempt to heat near x = 0 and sometime later turn on a beam in one computation. Still, a fairly complete scenario for this flare can be made from the results presented.

The thermal heating X-ray results in Figures 3-4 show a front moving out which would be consistent with Figure 1a,b from 22:32:29 to 22:32:57. Because the heating near x = 0 causes a slight density depression and the X-ray emission is proportional to n^2, the X-ray emission at 18 s has a peak away from x = 0. It is doubtful that this 10% variation could be detected with present spatial resolution.

The beam used in the beam heating results had $E_c = 20$ keV, $F = 10^{10}$ ergs cm^{-2} s^{-1}, and $\delta = 4$. The flux comes from DSS and δ from Dennis (private communication). This leads, using (Emslie 1978)

$$E = E_o\left[1 - \frac{3K\Lambda N}{E_o^2}\right]^{\frac{1}{2}}, \tag{4}$$

to the expectation that the maximum energy deposition will occur at $N = E_c^2/3K\Lambda = 3.5\times10^{19}$ cm^{-2} for $\Lambda = 28$ which is at x = 70,000 km. We see in Figure 2 that the maximum heating has occurred at 76,000 km at 14 s because some of the material in the flux tube has moved to larger x due to the heating by this time. The beam thermal X-ray signature in Figures 3-4 is quite small relative to the signature due to thermal heating.

In Figure 5 we have plotted the total X-ray signature of the beam including the nonthermal X-rays. In fact one can see by comparison of Figure 5 with Figures 3-4 that most of the emission is nonthermal emission. The physical reason is that the beam deposits energy over a large fraction of the loop so that the heating in one region does not raise the temperature a large amount over another region as is clear from Figure 2. Consequently the thermal emission is small. The nonthermal emission has a first peak around 73,000 km where the beam is depositing most of its energy. Intuitively one might guess that this is also the place from which the maximum emission dI/dx would occur (see, e.g., Brown and McClymont 1975). The reason that this is

not the case is that the photon energies are substantially below E_c and n rises steeply in the chromosphere. dI/dx is proportional to n/α^2, where $\alpha = 3K\Lambda N/E_c^2$, and the n factor increases much more rapidly than α^2 well beyond the place of maximum energy deposition.

Thus the beam X-ray emission should be concentrated near the footpoints, but will still be substantial to about 30,000 km above the footpoint. It should be kept in mind that the quantity plotted, dI/dx, must be integrated over the line of sight to obtain I. Nevertheless, there appears to be an order of magnitude discrepancy between the X-ray emission of the beam and the thermal X-ray emission (Figures 3-4 and Figure 5) with the same energy flux into both. The reason is that the beam energy is deposited over a relatively large area, keeping the thermal contribution small. We are investigating the effect of increasing the beam flux. DSS already concluded that the injected beam energy should be increased to obtain more evaporated material and, since they did not take into account scattering of beam electrons, their energy transfer was unrealistically efficient. Within the uncertainty of not having the results for higher beam fluxes, we feel that we have sufficient results to make a qualitatively, but not quantitatively, consistent scenario for this flare.

5. DISCUSSION

The results presented indicate the simplest manner of explaining the observations of Figure 1 with a minimum amount of injected energy. The observations from 22:32:29 to 22:32:57 can be explained by heating above footpoint B and the progressive expansion of a conduction front. An energy flux of 10^{10} erg cm^{-2} s^{-1} leads to temperatures and X-ray emission levels (Figures 2-4) consistent with the observations. The footpoint present at 22:33:06 can only be explained by a beam which was known to turn on about 22:32:50. A conduction front consistent with the observations from 22:32:29 to 22:32:57 could not have reached footpoint C at this time. Hence one cannot use the edge of the 2.2 counts s^{-1} contour to infer the position of a conduction front beyond 22:32:57 because of the contribution of the beam, a possibility already noted in RSS.

Thus, the velocity inferred on the basis of the 2.2 counts s^{-1} contour in RSS is too high. It is still less than the velocity obtained in Section 4 from the numerical results which is probably unrealistically high because the initial temperature is a factor 2 too low. Another effect which could be important in slowing the conduction front is the beam heating although it would not be important until after 22:32:48.

The observations from 22:33:06 to 22:33:25 can be explained by a combination of nonthermal X-rays from a beam, beam heating and the interaction of the conduction fronts from thermal heating and beam heating. Most of the extension of the 2.2 counts s^{-1} contour at 22:33:16 is due to beam heating and nonthermal X-rays. By 22:33:25 a conduction front is starting to move up from footpoint C which is consistent with the 6.7 counts s^{-1} contour and which could be made more pronounced in the numerical results by more beam heating. DSS noted that the amount of beam energy was uncertain by a factor ~4. Energy from thermal heating would then never be able to flow to footpoint C within the times in Figure 1 since the conduction front due to beam heating would

prevent the conduction front from B from traveling much beyond the center of loop BC. It is also possible to see, using equation (4), that energy in the 16-30 keV range as seen in Figure 2 of DSS for 30 s requires the injection of greater than 30 keV electrons. Beam heating could continue beyond 22:33:20 by the injection of lower energy electrons which would give no hard (16-30 keV) X-ray signature.

Thus, the most consistent interpretation of the observations in Figure 1 involves a combination of thermal waves and beam heating.

The author is grateful to Drs. Brian Dennis, Gordon Emslie, Alan Kiplinger, Marcos Machado and David Rust for helpful discussions. This work was supported by NASA contract NASW-3603 and NSF grant ATM-8314511.

REFERENCES

Brown, J. C., and McClymont, A. N. 1975, Solar Phys., 41, 135.
Brown, J. C., Melrose, D. B., and Spicer, D. S. 1979, Ap.J., 228, 592.
Duijveman, A., Somov, B. V., and Spektor, A. R. 1983, Solar Phys., 88, 257.
Emslie, A. G. 1978, Ap.J., 224, 241.
Emslie, A. G. 1980, Ap.J., 235, 1055.
Emslie, A. G., and Vlahos, L. 1980, Ap.J., 242, 359.
MacKinnon, A. L., Brown, J. C., and Hayward, J. 1985, Solar Phys., 99, 231.
Nagai, F., and Emslie, A. G. 1984, Ap.J., 279, 896.
Rust, D. M., Simnett, G. M., and Smith, D. F. 1985, Ap.J., 288, 401.
Smith, D. F. 1986, Ap.J., in press.
Smith, D. F., and Harmony, D. W. 1982, Ap.J., 252, 800.